Ab initio calculations of structural and electronic properties of gallium solid-state phases

M. Bernasconi* and Guido L. Chiarotti
International School for Advanced Studies, Via Beirut 2, I-34014 Trieste, Italy

E. Tosatti
International School for Advanced Studies, Via Beirut 2, I-34014 Trieste, Italy
and International Center for Theoretical Physics, P.O. Box 586, I-34014 Trieste, Italy
(Received 9 August 1994; revised manuscript received 22 March 1995)

Structural and electronic properties of various solid-state phases of gallium have been studied by means of first-principles total-energy calculations. Our results confirm that while the ground state α phase is characterized by the notable coexistence of metallic and covalent characters, the other phases are totally metallic. We predict that a phase transition from GaII to fcc should be observable at pressure ~ 150 kbar.

I. INTRODUCTION

Gallium is a trivalent metal with an unusual crystal structure in the stable low-pressure phase, called α-Ga. It has a rather complicated phase diagram with many stable and metastable crystalline phases all closely competing for the ground state. Two phases, GaII and GaIII,[1] are stable at high pressure. In addition, a number of metastable phases has been identified at atmospheric pressure designated β,[2] γ,[3] δ,[4] and ϵ.[1] The *Cmca* structure of the α phase is commonly described in terms of the face-centered orthorhombic unit cell with eight atoms per cell reported in Fig. 1.[5] A peculiar feature is that each atom has only one nearest neighbor at a distance 2.44 Å. The second, third, and fourth shells each contains two atoms, and are 0.27, 0.30, and 0.39 Å further apart. These six atoms can be seen as lying on a strongly buckled plane, about 1.9 Å thick, perpendicular to the [001] direction. Each atom in these strongly buckled planes is pairwise connected through a short bond to its first neighbor on the adjacent plane. The distance between nearest-neighbor atom pairs is comparatively short for a normal metallic bond, which foreshadow the covalent nature of this bond.[6,7] In the extreme covalent picture the Ga_2 pairs can be seen as dimers, making α-Ga the only elemental solid exhibiting both metallic and "molecular" character at zero pressure. The same *Cmca* structure is the ground state of the elemental molecular crystals Cl_2, Br_2, and I_2.[8] This behavior of Ga in the solid state, very different from that of its isoelectronic element Al, has been related by Jones[9] to a peculiarity of the Ga atom with respect to other elements in the same column. In gallium, the incomplete screening of the nucleus by a relatively shallow $3d$ core state yields an anomalous spatial contraction of the valence charge. This circumstance favors covalency over metallicity in Ga as though it were a much lighter element. In other words, Ga is closer to B than to Al.

Several physical properties indicate the partial covalent character of α-Ga. The thermal and electrical conductivities are highly anisotropic ($\sigma_c:\sigma_b:\sigma_a = 1:2.3:6.7$, for electrical conductivities), being lowest along the [001] direction, which is close to the direction of the Ga_2 dimers.[10] The optical reflectivity spectrum contains a sharp peak at a photon energy of 2.3 eV,[11,12] similar in shape to the bonding-antibonding transition in a semiconductor, such as Ge. The electronic density of states (DOS), derived from a photoemission experiment on polycrystalline α-Ga, shows a broad maximum 1.2 eV below the Fermi level (E_f) and an unusually steep decrease towards E_f,[13] suggesting a pseudogap. The presence of a pseudogap in the DOS at E_f is also consistent with the anomalous low value of the measured Knight shift.[14]

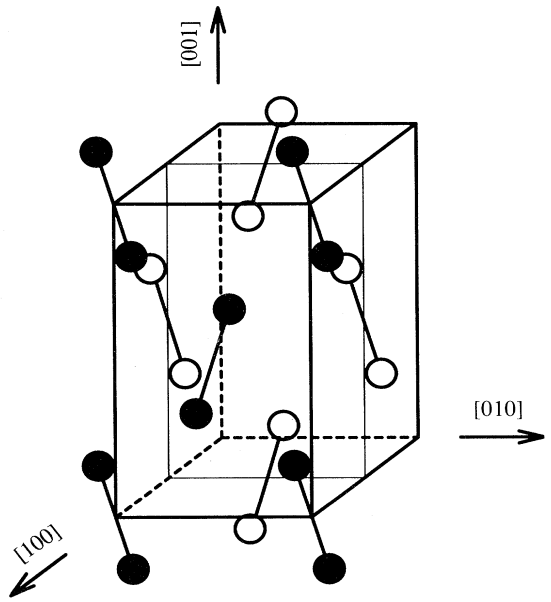

FIG. 1. Face-centered orthorhombic cell of α-Ga. Each site is occupied by a Ga_2 dimer. Filled circles represent atoms lying on the (100) plane at $x = a$, while open circle atoms lie on the next lower plane at $x = a/2$. Atoms in the $x = 0$ plane are in the same positions of those at $x = a$ and are not shown.

Theoretically a partial covalent character was first suggested by interpretations of the band-structure calculations based on empirical pseudopotentials.[6,11,15] The highest occupied and lowest unoccupied Σ bands along the [001] direction in fact show a remarkably low dispersion and are basically parallel and symmetric about E_f.

Further evidence for the covalent character of α-Ga, but not of liquid Ga, is obtained by comparing their transport properties. In liquid Ga, in fact, the conductivity is about a factor of 2 higher than σ_c in the crystal. This is the opposite behavior to that of regular metals, where conductivity drops at melting, due to higher scattering in the liquid phase. A behavior similar to α-Ga is found in most semimetals (Sb,Bi,Te) and is especially striking in group-IV elements, such as Si or Ge, whose solids are covalently bonded, while their metals are metallic. Moreover, as in Si and Ge, the density of gallium in the liquid phase is higher than in the crystalline phase: the corresponding change in specific volume is about 3.2%.[17] Finally the low-temperature structure factor $S(k)$ of liquid Ga shares some covalent features with those of Si and Ge, in particular, a shoulder of $S(k)$ at about 3 Å^{-1}, which lies on the high-momentum side of the first and main peak.[18] No such shoulder is found instead in the isoelectronic liquid metals Al, In, and Tl,[18] which do not posses a stable covalent phase. The origin of this shoulder and its relationship with the covalent nature of α-Ga have been recently addressed via *ab-initio* simulations by Gong *et al.*[19] Although the electronic properties of liquid Ga are similar to those of β-Ga, covalency manifest itself in the appearance of very short-lived Ga-Ga bonds, which represent the remnants in the liquid of the Ga_2 dimers in crystalline α-Ga.

The covalency of the dimer and its fingerprint in the electronic properties, in particular the presence of a pseudogap at the Fermi level in the electronic densities of states, has been recently confirmed by first-principles calculations by Gong *et al.*[20] and Hafner and Jank.[21] Gong *et al.*[20] also found a good agreement between theoretical prediction and experimental data on electronic band structure and optical conductivity.

In the following we present new *ab-initio* results on the structural and electronic properties of the phases α-Ga, β-Ga, GaII, GaIII, and for a hypothetical fcc phase. This new set of calculations is more accurate than that previously published in Ref. 20, and supersede them, particularly in the resulting energy heirarchy of the various phases, which is very delicate. The main properties and conclusions drawn in Ref. 20 remain altogether correct.

The zero-temperature theoretical phase diagram of Ga derived by these calculations as a function of pressure is as follows. Starting from the α phase at zero pressure, a transition to GaII is found at $\sim$50 Kb, in agreement with experimental data.[1] A second, new transition from GaII to fcc is predicted at 145 Kb. On the other hand, the GaIII and β phases are not reachable by pressure at $T=0$. Among the other phases, β-Ga is the lowest in energy above the ground state.

This paper is organized as follows: In Sec. II we describe the computational method, with particular focus on accuracy problems. In Sec. III we discuss the structural properties and the relative stability of the various phases. We have found a systematic error of $\sim$10% in the equilibrium volume of all phases. For this reason we have checked the possible importance of corrections to both the pseudopotential approximation, including the nonlinear core correction (NLCC), as well as the gradient correction (GC) to the simple local-density approximation (LDA). How these corrections affect the structural properties is discussed in Sec. IV, where, however, we read the conclusion that they do not improve the misfit.

Finally in Sec. V we discuss the electronic properties of the various phases, and Sec. VI is devoted to conclusions.

II. COMPUTATIONAL METHOD

We have studied structural and electronic properties of bulk gallium phases within the *ab-initio* total-energy framework, via the standard density functional theory in the LDA. Our chosen local exchange and correlation (xc) energy is that of Perdew and Zunger.[22] The norm-conserving pseudopotential for Ga was taken in the Kleinman-Bylander (KB) form,[23] built from the tables of Stumpf, Gonze, and Scheffler.[24] This pseudopotential is constructed by linearizing the xc energy with respect to valence and core contributions, i.e., in the applications of the pseudopotentials the xc energy is computed using only the (pseudo)valence charge density. This approximation is usually well suited when the overlap between core and valence charges is small. In view of the anomalous atomic properties of Ga discussed in the Introduction, it may be expected that the pseudopotential description of solid Ga could be somewhat more delicate than for, e.g., Al. In order to test this point explicitly we have generated a pseudopotential with the nonlinear core correction (NLCC), according to the prescriptions suggested by Louie, Froyen and Cohen.[25] This amounts to evaluating the xc energy using the total—rather than the valence—charge density, and is achieved by adding the frozen-core charge to the self-consistent valence charge. The NLCC pseudopotential has been generated in the von Barth and Car form.[26,27] Furthermore, we checked the possible importance of corrections to standard LDA. We recomputed the structural properties of α-Ga using a gradient correction (GC) to the xc functional. For this, we adopted the semiempirical exchange correction of Becke[28] and the correlation correction of Perdew[29] (BP), and we used the gradient-corrected pseudopotential generated by Ortiz[30] according to the prescription given by Ortiz and Ballone.[31] Kohn-Sham orbitals were expanded in plane waves up to an energy cutoff of 14 Ry for the KB and the GC pseudopotentials and up to 18 Ry for the NLCC pseudopotential, which requires a higher cutoff for the description of the frozen-core charge.

The closeness in energy of the different crystalline phases of gallium requires a very high-accuracy Brillouin-zone (BZ) integration in order to correctly reproduce the heirarchy of the different structure. Previous work done in our group on bulk gallium,[20] although properly reproducing the electronic properties of α-Ga, did not correctly predict this hierarchy, and, consequently, the pressure-induced phase transitions, due to poor ac-

curacy in the BZ integration. For this reason, we devised a high-precision BZ integration following the scheme proposed by Methfessel and Paxton.[32] It consists in a modification of the more popular Gaussian smearing technique of Fu and Ho[33] and is described in the Appendix. Requiring an accuracy within 3 meV/atom in the bulk total energy of the different phases, we used the following numbers of k points in the irreducible BZ (IBZ): $N_{\mathbf{k}}=27,256,55,512,203$ spreading parameters $w=20,50,70,70,70$ mRy, and $n=0,5,2,2,2$ for the α, β, GaII, GaIII, and fcc phases, respectively.

The structure of each phase is determined by a set of lattice and internal parameters. In α-Ga, for instance, there are the three lattice parameters a,b,c of the orthorhombic cell, and two internal degrees of freedom, which control the bond length and orientation of the Ga_2 dimer. For all the phases studied we found the full set of equilibrium structural parameters, which minimize the total energy at each volume by calculating forces and stress from the self-consistent wave functions by means of Hellman-Feynman[34] (HF) and stress[35] theorems.

At each fixed volume preliminary calculations were performed with different values of the lattice parameters. The number of such preliminary calculations at each volume was equal to that of the lattice parameters. For each choice of lattice parameters the internal degrees of freedom were optimized by relaxing the atomic positions inside the unit cell guided by the HF forces. We then deduced the equilibrium values of the lattice constants for each volume by a linear extrapolation of the anisotropic part of the stress tensor (i.e., $\sigma_{xx}-\sigma_{yy}$ and $\sigma_{xx}-\sigma_{zz}$ for α-Ga or $\sigma_{xx}-\sigma_{zz}$ for the tetragonal GaIII, x, y, and z being along the crystallographic axes). The residual anisotropy in the stress was less than 1 kbar for α-Ga and GaIII, and 10 kbar for β-Ga which is more difficult, requiring the optimization of four lattice parameters [a, b, c, and $\cos(ac)$]. The β-Ga structure near the equilibrium volume, however, was also further refined with a residual anisotropy in the stress less than 1 kbar.

III. STRUCTURAL PROPERTIES

The experimental phase diagram of gallium[1] reproduced in Fig. 2 shows stability regions for solid α-Ga, GaII, and GaIII phases. Many other metastable phases, named β, γ, δ, ϵ, are also experimentally observed.[1] α-Ga is the stable phase at ambient pressure, while two other phases are stable at high pressure and/or temperature: GaII and GaIII. β-Ga is a metastable phase obtained by supercooling the liquid[2] or by heating amorphous Ga,[37] obtained in turn by deposition of the vapor onto a cold substrate.[38] Bosio[1] pointed out that GaIII may be prepared in a metastable state below the liquid-α-GaII triple point by compressing or cooling the liquid. At 40 kbar GaIII may be supercooled by as much as 80–100 K before it transforms to GaII. In previous studies of the crystal structure of Ga at high pressure[36,39] these metastability phenomena were not known, and the phase reached from α-Ga under hydrostatic pressure was erroneously identified with the face-centered-tetragonal

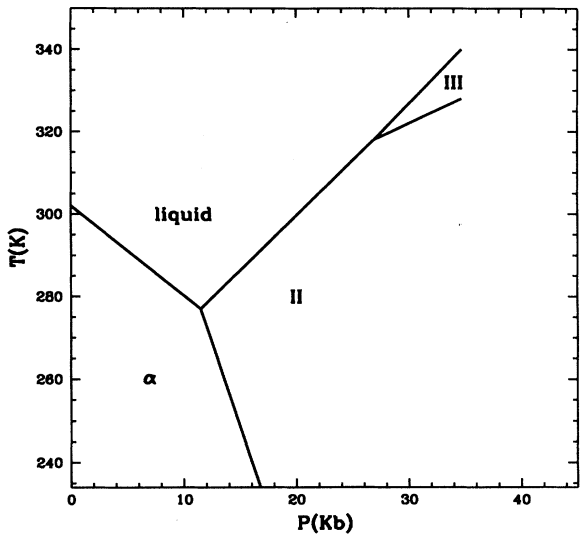

FIG. 2. Phase diagram of Ga from Ref. 1.

structure of GaIII. Following these older results, Gong *et al.*[20] studied the zero-temperature pressure-induced phase transition α-Ga$\rightarrow$GaIII (named GaII there, as in older literature) and ignored instead the true structure of GaII, and then the true transition α-Ga$\rightarrow$GaII, discovered by Bosio.[1]

The $Cmca(D_{2h})$ structure of α-Ga is shown in Fig. 1, the dimers pictured as dumb bells. The bond length and orientation of each dimer are controlled by two internal degrees of freedom denoted as u and v. The structure is thus determined by five parameters: a, b/a, c/a, u, and v. The positions of the eight atoms in the orthorhombic unit cell (twice as large as the primitive cell) are functions of u and v in the form[5]

$$(0,u,v) \quad (\tfrac{1}{2},u,\tfrac{1}{2}+v) \quad (\tfrac{1}{2},\tfrac{1}{2}+u,-v) \quad (0,\tfrac{1}{2}+u,\tfrac{1}{2}-v)$$
$$(0,-u,-v) \quad (\tfrac{1}{2},-u,\tfrac{1}{2}-v) \quad (\tfrac{1}{2},\tfrac{1}{2}-u,v) \quad (0,\tfrac{1}{2}-u,\tfrac{1}{2}+v)$$

with the experimental values $u=0.0785$ and $v=0.1525$ (x,y,z, are intended to be multiplied by a, b, c, respectively). The primitive unit cell of C-centered monoclinic β-Ga, space group $C2/c(C_{2h})$, contains two atoms at $\pm(0,y,\frac{1}{4})$ with $y=0.131$ at 248 K.[2] Figure 3

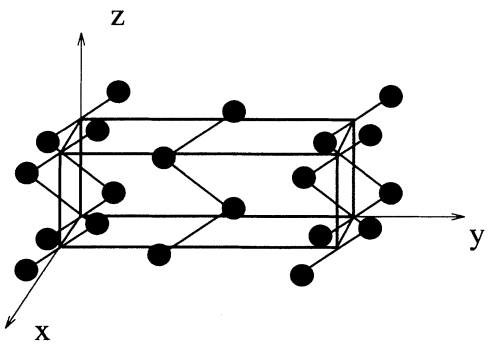

FIG. 3. Conventional monoclinic cell of β-Ga. The nearest-neighbor atoms forming chains along [0,0,1] are connected by lines.

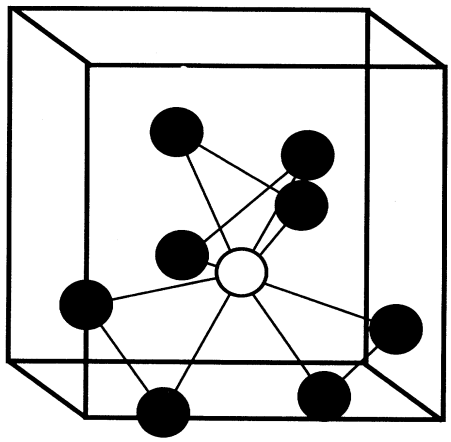

FIG 4. Nearest-neighbor environment in GaII. A particular atom (empty circle) in the conventional cubic cell and its eight nearest neighbors (filled circle) are depicted. Nearest-neighbor atoms are connected by lines.

shows the conventional monoclinic cell of β-Ga.

GaIII is face centered tetragonal,[1] similar in structure to indium, and has only two structural parameters: a and c/a.

GaII is body centered cubic (Td point group) with six atoms in the unit cell at[1]

$$\begin{array}{lll} (\tfrac{3}{8},0,\tfrac{1}{4}) & (\tfrac{1}{4},\tfrac{3}{8},0) & (0,\tfrac{1}{4},\tfrac{3}{8}) \\ (\tfrac{1}{8},0,\tfrac{3}{4}) & (\tfrac{3}{4},\tfrac{1}{8},0) & (0,\tfrac{3}{4},\tfrac{1}{8}) \,. \end{array}$$

Each atom has eight nearest neighbors as depicted in Fig. 4. The metastable phases δ[4], and γ[3] whose unit cells contain 40 and 22 atoms, respectively, and the phase ϵ, whose structure has not been determined yet, are not considered here any further. All experimental values of the lattice parameters of α, β, GaII, and GaIII are collected in Table I.

In Fig. 5 we plot the energy versus volume per atom of the various phases calculated with the KB pseudopotential and the simple LDA. The points were obtained by allowing a full relaxation of atomic positions inside the unit cell and by optimizing the lattice constants at each volume by using the calculated stress tensor as discussed in Sec. II. The zero-point vibrational energy is not included. The points have been interpolated with Murnaghan's equation of state.[40] The theoretical lattice parameters at the equilibrium volume are compared with the experimental data in Table I. The theoretical internal degrees of freedom at equilibrium for α-Ga are $u=0.0803$, and $v=0.1567$ [experiment: $u=0.0785$ and $v=0.1525$ (Ref. 5)], while the internal parameter y in β-Ga is $y=0.134$ [experiment: $y=0.131$ (Ref. 2)]. The theoretical bulk modulus B_0 and its pressure derivative at the equilibrium volume B_0' are reported in Table II. The experimental bulk modulus is known only for α-Ga, $B_0^{\text{expt}}=613$ kbar at 4.2 K and atmospheric pressure.[41] The agreement with the theoretical value (669 kbar) is good. The theoretical equilibrium volume is $\sim 10\%$ smaller than the experimental one for all phases.[42] The other structural parameters are, however, in excellent agreement with experimental data (error $<2\%$). Figures 6(a)–6(c) report the dependence of b/a, c/a, and of the dimer bond length (d_{dimer}) on the volume of α-Ga. Both b/a and c/a increase with pressure (the small oscillations at volumes in the range 110–120 a.u. are due to numerical noise). The line in Fig. 6(c) represents the ideal scaling of the dimer bond length, i.e., $d_{\text{dimer}} \sim 0.929 V^{1/3}$, where 0.929 is the ratio $d_{\text{dimer}}/V_0^{1/3}$ at equilibrium. This line interpolates our results rather well, indicating that the Ga-Ga distance in the dimer varies with the volume as the average Ga-Ga distance. In the previous work by Gong *et al.*[20] the slope of the straight line interpolating their results was 20% lower than the ideal value, but there the ratio of the lattice parameters was fixed at the experimental value and not allowed to vary with pressure. Actually the c/a, and b/a ratios have a non-negligible variation with volume as reported in Figs. 6(a) and 6(b). The equilibrium energy per atom, calculated with the LDA and KB pseudopotential, of α-Ga, β-Ga, GaII, GaIII, and fcc phases are -4.5128, -4.5094, -4.5085, -4.5075, and -4.5074 Ry/atom, respectively. All phases lie within a narrow energy window, 6 mRy/atom large. Although the α-Ga structure had been found as the stable phase also in older calculations within pseudopotential perturbation theory,[6,7,44] the exact hierarchy in energy of the other phases, and the related pressure-induced phase transitions, differ widely in

TABLE I. Theoretical (LDA) and experimental lattice constants (a.u.) of different phases of gallium. The experimental data are taken from Ref. 5 for α-Ga (4.2 K, and atmospheric pressure), from Ref. 1 for GaII (at 313 K and 26 kbar), from Ref. 1 for GaIII (at 298 K and 28 kbar), and from Ref. 2 for β-Ga (at 248 K and atmospheric pressure). The small deviation from orthorhombic symmetry in β-Ga is accounted for by the angle β between the a and c axes. We obtained $\beta=92.45°$, while the experimental value is $\beta=92.03°$.

Phase	Theory				Expt.			
	a	b/a	c/a	Vol.	a	b/a	c/a	Vol.
α	8.271	0.994	1.688	119	8.523	1.0013	1.695	131
β	4.954	2.973	1.218	111	5.227	2.911	1.205	125
GaII	10.937			109	11.246			119
GaIII	7.312		1.110	109	7.518		1.119	119
fcc	7.571			108				

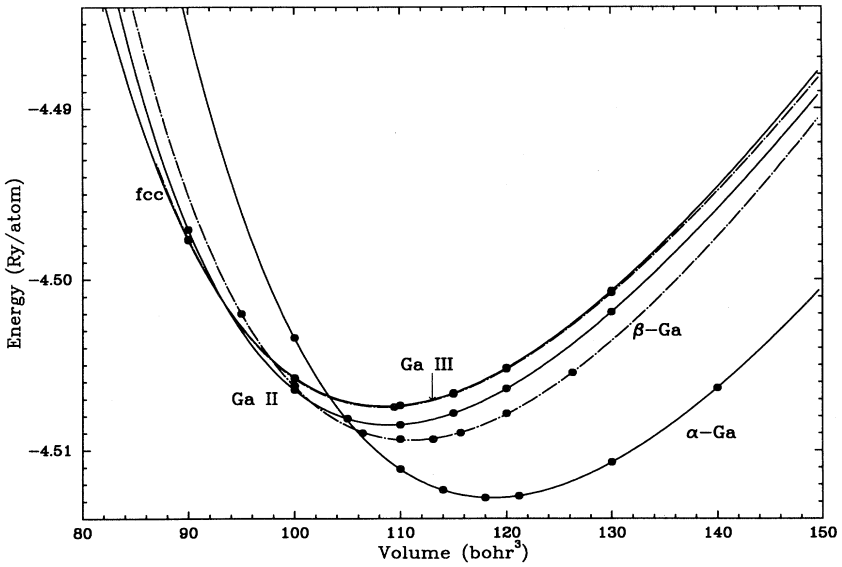

FIG. 5. Equation of state of five phases of Gallium at $T=0$, calculated in LDA. The zero-point vibrational energy is not included. The equation of state of GaIII (dashed-dotted lines) ends at 87 a.u. (see text).

different calculations, depending on the choice of pseudopotentials and dielectric functions. In our calculation the phase closest to α-Ga is β-Ga, as one might expect from the wide metastability region of the latter phase and from its high melting temperature [$T_m(\beta)=257$ K, against $T_m(\alpha)=303$ K]. Moreover, the density of β-Ga, being 7% higher than that of α-Ga at equilibrium, is closer to that of liquid gallium, consistent with the easy growth of β-Ga from the supercooled liquid.

The phase reached by α-Ga under hydrostatic pressure is GaII, in agreement with experimental evidence.[1] Our theoretical transition pressure is $P_{\alpha\text{-GaII}}=64$ kbar. Inclusion of the zero-point energy in the Debye approximation decreases the transition pressure to ~ 50 kbar.[45] The experimental transition pressure at $T=0$ K can be obtained by extrapolating the α-Ga/GaII coexistence line in Fig. 2. This gives an upper bound of 48 kbar. A better estimate is obtained by taking the linear extrapolation down to about one-fifth of the Debye temperature (240 K), giving 41 kbar. Both values compare well with our theoretical result. At higher pressure, a new phase transition from GaII to fcc is predicted at 145 kbar. Since both GaII and fcc are fully metallic phases and have similar compressibility, we expect for them a similar Debye temperature and therefore a negligible effect of the zero-point energy on the GaII→fcc transition pressure. As far as we know this region of pressure has not yet been explored experimentally. Thus, we propose that the phase diagram in Fig. 2 should be enriched with the new coexistence line GaII-fcc, which could continue also in the GaIII region as a GaIII-fcc coexistence line. Indeed we found that GaIII is mechanically unstable for pressures higher than 250 kbar. For a fixed equilibrium volume higher than 87 a.u. (pressure lower than 250 kbar) the energy per atom as a function of the c/a ratio has two minima: one at $c/a=1$ corresponding to the ideal fcc, and the other for c/a in the range 1.05–1.18 corresponding to GaIII. By increasing the pressure, the GaIII minimum is increasingly shallow and shifts to a smaller c/a ratio. Finally for volumes less than 87 a.u. ($P>250$ kbar) the minimum in the $E=E(c/a)$ curve corresponding to GaIII disappears, and only the minimum at $c/a=1$ (fcc) survives, therefore indicating the mechanical instability of GaIII in this pressure range.

IV. GRADIENT CORRECTION AND NONLINEAR CORE CORRECTION EFFECTS ON STRUCTURAL PROPERTIES

The theoretical equilibrium volume is $\sim 10\%$ lower than the experimental one for all phases (cf. Table I). While a certain tendency to overestimate the atomic density is common to most LDA calculations, this error is somewhat larger than usual. In order to estimate if our neglect of the core charges plays a role in this misfit, we recomputed the equation of state for α-Ga, GaII, and fcc with a new pseudopotential including the NLCC. The new structural parameters are reported in Table III. From Table III we can see that the NLCC does not improve the misfit in the equilibrium volumes. The other

TABLE II. Theoretical (LDA) bulk modulus (B_0, in kbar) and its pressure derivative (B_0', dimensionless) at the equilibrium volume for the different phases. The experimental bulk modulus is known only for α-Ga, and it is equal to $B_0^{\text{expt}}=613$ kbar at 4.2 K and atmospheric pressure (Ref. 41).

	α	β	GaII	GaIII	fcc
B_0 (kbar)	669	700	676	637	637
B_0'	4.683	4.735	5.034	4.652	4.414

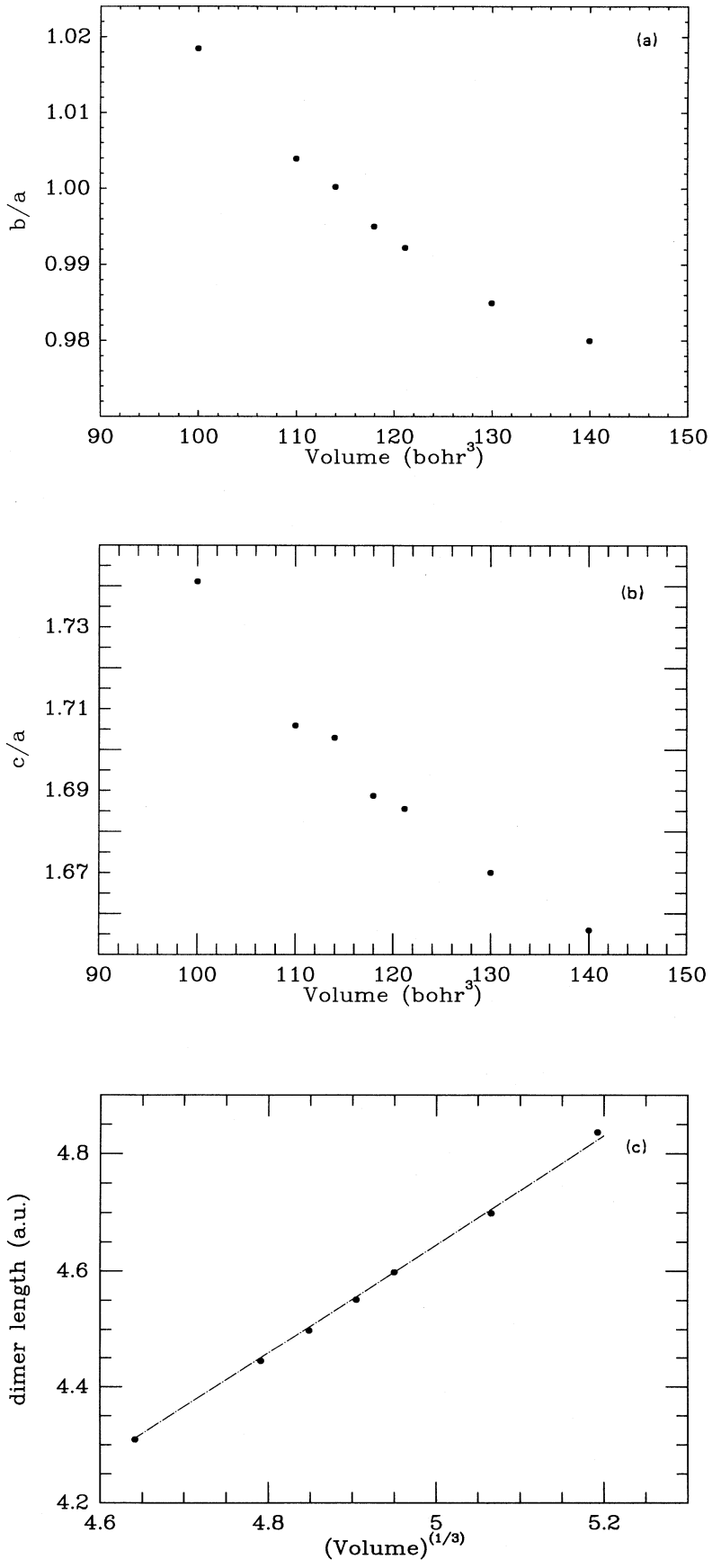

FIG. 6. Dependence on the α-Ga volume of the theoretical (LDA) structural parameters (a) b/a, (b) c/a, and (c) the dimer bond length. In figure (c) the dotted line corresponds to the "ideal" bond length scaling $V^{1/3}$. Its slope is 0.929, equal to $d_{\text{dimer}}/V_0^{1/3}$ at the equilibrium volume.

TABLE III. Structural parameters in a.u.; bulk modulus and its pressure derivative for α-Ga, GaII, and fcc phases at the equilibrium volume calculated with a NLCC pseudopotential.

	Theoretical lattice parameters with NLCC							
Phase	a	b/a	c/a	Vol.	u	v	B (kbar)	B'
α	8.290	1.0013	1.695	121	0.0814	0.1573	669	4.928
GaII	10.97			110			709	5.099
fcc	7.590			109			676	4.633

structural parameters are only slightly modified by the change of the pseudopotential except for the transition pressures which undergo large variations. $P_{\alpha\text{-GaII}}$ is reduced to 38 kbar (64 kbar without NLCC), and $P_{\text{GaII-fcc}}=98$ kbar (145 kbar without NLCC). These variations are mainly because of the change in the relative energies of the three phases; in fact, an error of 3 meV in the energy difference between GaII and fcc induces an error of 30 kbar in $P_{\text{GaII-fcc}}$. The main message of this result is that the neglect of NLCC is not the source of the error in the equilibrium volumes. This misfit is more likely a failure of the LDA, well known to overbind molecules[46] and to overestimate bulk moduli and equilibrium densities, in the solid state. Indeed, the LDA length of the Ga_2 dimer in the α phase at the experimental equilibrium density is 2.485 Å, $\sim$2% larger than the experimental value 2.44 Å both with and without NLCC. Hence the LDA tends to favor charge homogeneity, reducing the difference in strength between the intradimer and interdimer bonds. In fact, at the equilibrium volume of 121 a.u. (NLCC result), for instance, the theoretical phonon frequencies of the low-energy normal modes modulating the interdimer bonds (vibrations of the dimers) are overestimated, while the frequencies of the higher-energy stretching modes of the dimer are underestimated (5–10 % error),[48] although the theoretical volume is 8% smaller than the experimental one. At the experimental equilibrium volume the misfit between theoretical and experimental phonon frequencies increases further. Details in the *ab-initio* phonon spectrum of α-Ga will be published elsewhere.[48]

In order to improve over simple LDA we recomputed the structural properties of the phase α with the BP gradient-corrected functional (see Sec. II). The GC does expand the equilibrium volume of α-Ga, which becomes 132 a.u., (experiment: 131). This is a general property of the GC functionals, which favor charge inhomogeneities and consequently expand the lattice constants.[49] However, the GC underestimates the bulk modulus in α-Ga, which drops as low as 503 kbar (experiment: 613 kbar). At the same time, it does not improve the length of the dimer, which is still 2% larger than the experimental value. Moreover, the phonon frequencies are decreased in the GC calculation, and the overall agreement with experimental data is worse than in the LDA calculation, indicating that the balance between stronger and softer bonds does not improve with the GC. In summary, the residual misfit in the LDA structure calculation is not seriously improved by the NLCC nor by the GC. Thus, in the following we shall give the results on the electronic properties calculated with the simple LDA functional and the KB pseudopotential without NLCC. Our results suggest that the presence of a competition between covalent and metallic bonds make gallium a particularly severe system to test the validity of xc functionals.

V. ELECTRONIC PROPERTIES

The electron (pseudo)charge density of α-Ga is compared to those of the other phases in Fig. 7. The molecular Ga_2 short bond in α-Ga gives rise to a pile up of charge in the center of the dimer. Conversely in all the other phases the distribution of charge is smeared but otherwise atomiclike with a maximum of charge near each atom and not midway between the atoms. The maximum of (pseudo)charge density in the dimer covalent bond is $\sim$0.058 a.u., comparable to the corresponding value on the covalent bond of germanium 0.0742 a.u.[50]

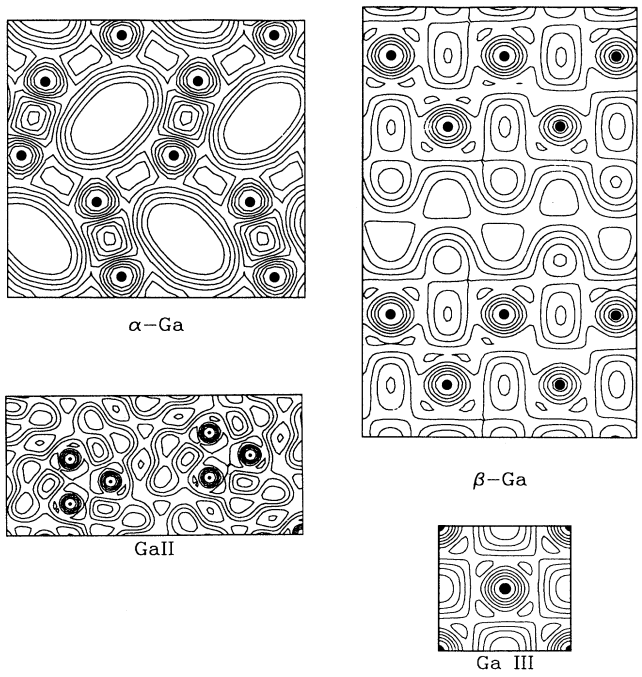

FIG. 7. Electron (pseudo)charge density map of the different phases of gallium computed at the equilibrium volume of each phase. The contour lines are separated by 0.005 a.u. α-Ga and β-Ga charge densities are plotted on the (100) plane. GaIII charge density is plotted on the (001) plane. GaII charge density is plotted on the plane passing through the atoms of the trimers shown. The scale is half those of the other pictures. The trimers are formed by one central atom and by two other atoms in its first-neighbor shell.

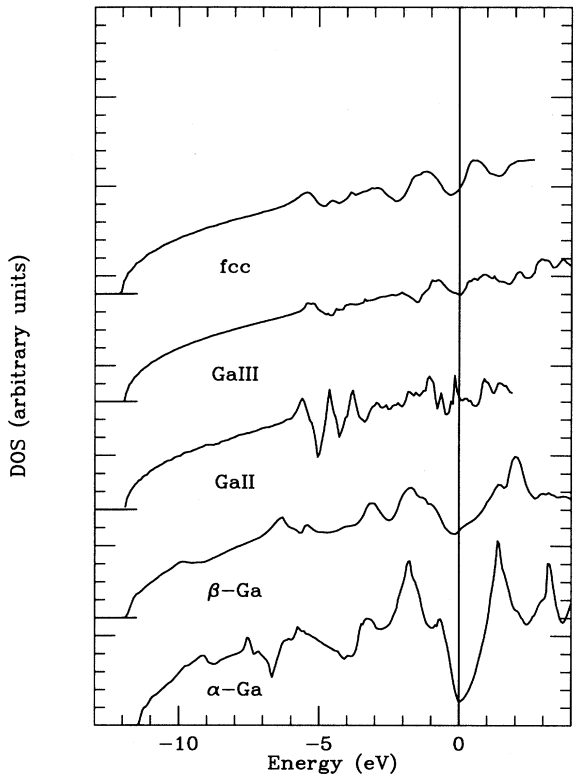

FIG. 8. Electronic density of states of the different phases of gallium, calculated at the equilibrium volume of each phase by using a uniform mesh in the IBZ including up to 300 k points. The tetrahedron linear analytic interpolating method has been used (Ref. 51).

The partial covalent character of α-Ga and the fully metallic nature of the other phases is even more apparent in the electronic density of states (DOS) of Fig. 8. The DOS of α-Ga is rather structured and shows a pronounced pseudogap at the Fermi level, in agreement with earlier calculations[20,21] and with photoemission studies.[13] The connection between the pseudogap and covalency in α-Ga was discussed long ago by Heine.[6] The residual states in the pseudogap are mainly related to the overlap of the electronic wave functions along the buckled planes perpendicular to the molecular bond. These states lead to metallic behavior, which thus coexists with the molecular state. S-like states, localized in the buckled planes, are also the main contribution to the density of states from the bottom of the valence bands (~ -12 eV) up to -6.5 eV below the Fermi level. The coexistence of two kinds of bonding, covalent and metallic, apparently contributes to the stability of this structure. The fact that the states in the gap are related to the in-plane electron motion is also suggested by the band structure of Fig. 9, very close to that previously published by Gong *et al.*[20] The strong anisotropy at the Fermi surface indicates preferential conduction along the (001) planes in agreement with experiment. Details of the electronic structure at the Fermi level,[15,16] such as the small hole pocket in the T direction, are brought out well. We also note the presence of roughly parallel bonding-antibonding pairs of bands nearly symmetric with respect to the Fermi level, typical of covalent materials. Gong *et al.* have shown that the gap (~ 2.3 eV) between these parallel bands, indicated by the arrows in Fig. 9, is directly connected to a strong peak in the optical conductivity. This is a rather unusual feature for a metallic system and, in fact, reflects

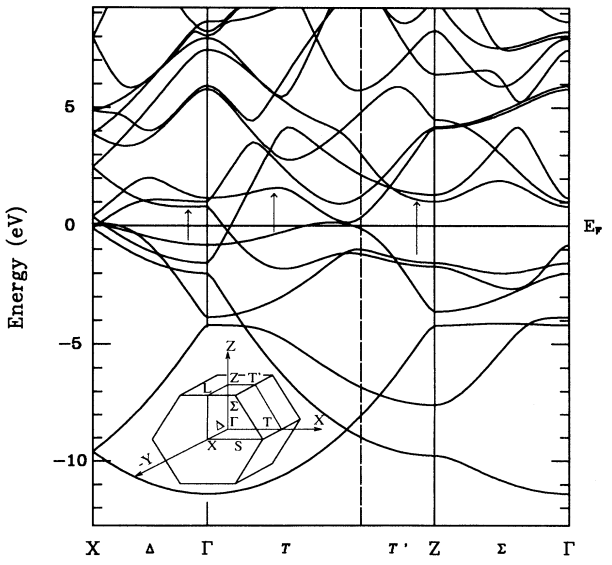

FIG. 9. The band structure of α-Ga along some high-symmetry lines in the Brillouin zone. Arrows denote important bonding-antibonding optical transitions.

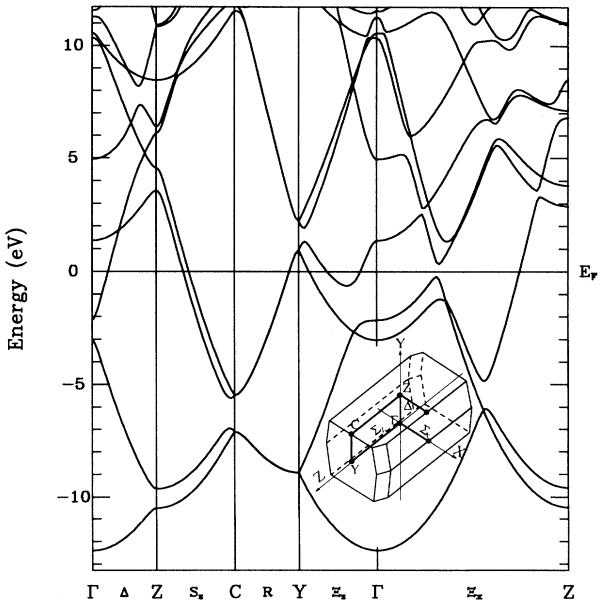

FIG. 10. The band structure of β-Ga along some high-symmetry lines in the Brillouin zone. In the figure of the Brillouin zone the scales in the three directions have been modified to clarify the view, and the difference between angle β and 90° has been exaggerated.

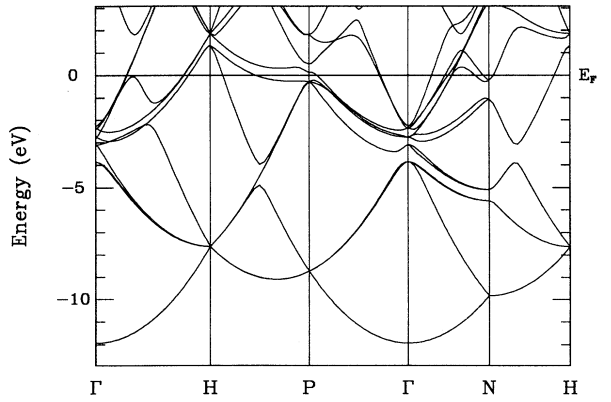

FIG. 11. The band structure of GaII along some high-symmetry lines in the bcc Brillouin zone. Points are labeled following Zak (Ref. 52).

directly the bonding→antibonding transition of the Ga_2 covalent molecule. The antibonding character of the states, which mostly contribute to the peak in the DOS just above E_F, is confirmed by direct inspection of our KS orbitals. The agreement between the experimental $\sigma(\omega)$ (Refs. 11 and 12) and that calculated in Ref. 20 is good (cf. Fig. 4 in Ref. 20), indicating that LDA theory correctly reproduces the electronic properties of α-Ga, down to a very considerable detail.

Coming now to the other phases, we plot their electronic bands along some high-symmetry lines in the IBZ in Figs. 10–13. We note that GaIII, β-Ga, and fcc-Ga have a very similar DOS, nearly free-electron-like in the low-energy range, and with a large value at the Fermi level, consistent with their good metallic properties. In particular, since GaIII is tetragonally distorted fcc, its electronic densities and bands are very similar to those of fcc-Ga. Conversely the GaII phase still presents some structures in the DOS around 4–5 eV below the Fermi level. The large difference between the DOS at the Fermi level $[D(E_F)]$ of α-Ga and β-Ga is experimentally reflected in the Knight shift, which in β-Ga is about three times larger than in α-Ga.[14] We obtained a ratio of about 3.5 between the calculated values of $D(E_F)$. Although we have not attempted to estimate the relative values of $|\Psi(0)|^2$ between α-Ga and β-Ga, the pseudocharge densities near the s core radius ($r_s = 1.72$ a.u.) are not dissimilar, which suggests that the difference in $D(E_F)$ is indeed the main factor.

Finally we recall that Gong *et al.*, in order to suggest some direct method to detect the covalent bond, compared in Ref. 20 the electronic structure factor calculated in two different ways: the first $[S_c(\mathbf{k})]$ using the true electronic (pseudo)charge density and the second $[S_a(\mathbf{k})]$ using a superposition of atomic charges. $S_c(\mathbf{k})$ and $S_a(\mathbf{k})$ show an overall similar behavior, apart from a close multiplet K^* of reciprocal lattice vectors ([113] [121] [022] [004]), which is enhanced in $S_c(\mathbf{k})$. However, here the

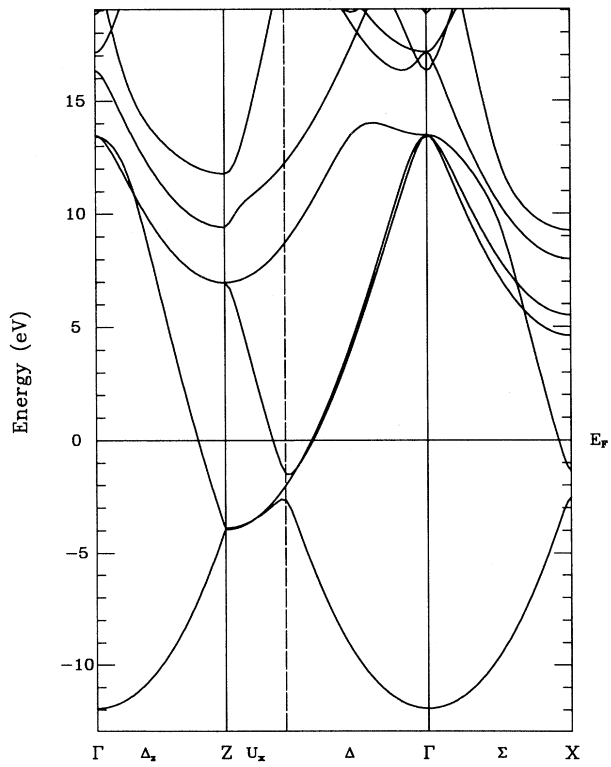

FIG. 12. The band structure of GaIII along some high-symmetry lines in the Brillouin zone. Points are labeled following Zak (Ref. 52).

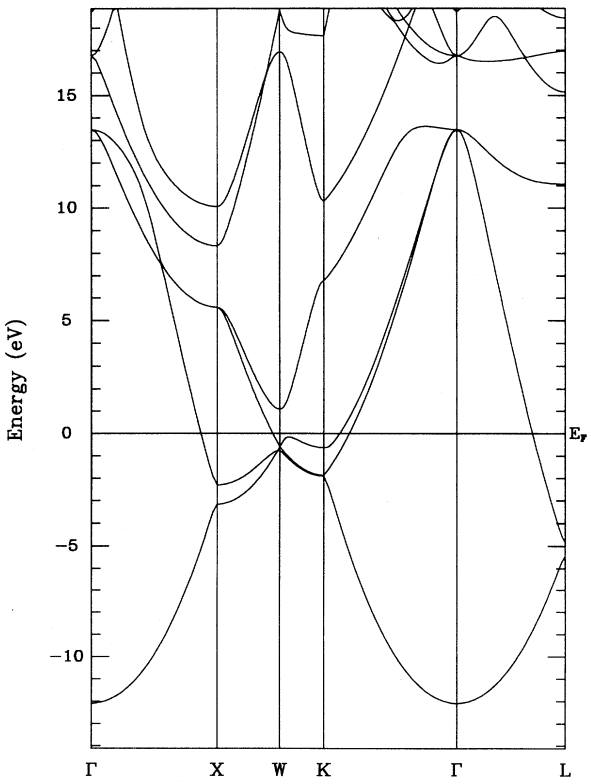

FIG. 13. The band structure of fcc-Ga along some high-symmetry lines in the Brillouin zone. Points are labeled following Zak (Ref. 52).

situation is different from diamond, where the presence of the covalent bond gives rise to a forbidden reflection at $(2\pi/a)(222)$, and its presence is thus directly confirmed by x-ray measurements.[53] In the case of α-Ga the reflection at the K^* multiplet is not forbidden by symmetry, as shown by the presence of a (small) contribution to the K^* multiplet from $S_a(\mathbf{k})$.[20] For this reason, if one includes core electrons in the calculation of the electronic structure factor, as should be done for a comparison with x-ray intensities, the difference between $S_c(\mathbf{k})$ and $S_a(\mathbf{k})$ becomes much less pronounced, being of only few percent at the K^* multiplet, and almost impossible to detect experimentally. Thus, we need to rectify the suggestion in Ref. 20 that x-ray measurements can easily confirm the presence of a covalent bond in α-Ga.

VI. CONCLUSIONS

The simultaneous presence of two kinds of bonding makes gallium a metal with peculiar properties. Our calculations essentially reproduce the previous *ab-initio* results[20,6] on the semimetallic phase α, showing a pile up of charge in the Ga_2 dimer characteristic of a covalent bond and its fingerprint in the electronic properties, as a pronounced pseudogap in the electronic density of states at the Fermi level. However, the heirarchy in energy of the other structures is improved in our refined calculation, and now accounts well for the experimental results on gallium phase diagram. In particular, the phase reached by α-Ga under hydrostatic pressure is the GaII phase of Bosio.[1] In addition, we predict a new phase transition from GaII to fcc at higher pressure.

The structural properties of the gallium phases are satisfactorily reproduced by our calculation. However, some discrepancies in the structure still persist and induce 5–10 % errors in the phonon frequencies.[48] In particular, the length of the dimer is 2% larger than the experimental value at the experimental equilibrium volume, and this misfit does not improve by including either the nonlinear core correction to the pseudopotential or the gradient correction to the xc functionals. The presence of competition between covalent and metallic bonds make gallium a particularly severe system to test the validity of xc functionals. Both the LDA and the BP gradient corrections tested seem to favor charge homogeneity and to make the shorter intradimer and the large interdimer bonds more similar. One additional source of error in our calculations, which might be connected with the misfit in the equilibrium volumes, is an involvement of the core $3d$ electrons, frozen in our pseudopotential framework. This effect should be further studied via an all-electron LDA calculation.

We have provided a unifying interpretation of the many indirect experimental evidences of the presence of the covalent bond in the dimer. Unfortunately a direct experimental signature of the bond charge in x-ray measurements is unlikely. In fact, contrary to the cases of IV semiconductors, the reflections magnified by the presence of the bond charge are symmetry allowed. The presence of the covalent bond can therefore be further confirmed only indirectly. Its signature is also visible in the phonon spectrum deduced from the neutron-scattering data of Ref. 54: The flat phonon branches around 7 THz, separated by a 1-THz gap from the other branches, corresponds to strong (covalent) dimer-bond stretching, as shown by a recent *ab-initio* calculation.[48] In the fully metallic β-Ga phase the corresponding feature in the phonon density of states is, instead, absent.[55] Moreover, the covalent bond is expected to play a crucial role in the physics of α-Ga surfaces recently studied experimentally with scanning-tunneling microscopy[56] and theoretically within the same total-energy framework presented here.[57,58]

ACKNOWLEDGMENTS

We are grateful to S. Baroni, M. Buongiorno Nardelli, A. Dal Corso, and P. Giannozzi for providing us with their DFT Fortran library. We acknowledge support by the Italian Consiglio Nazionale delle Ricerche through Progetto Finalizzato Sistemi Informatici e Calcolo Parallelo and through SUPALTTEMP, by INFM, and by EEC through Contract Nos. ERBCHBGCT920180 and 940636, as well as ERBCHRXCT930342.

APPENDIX: k-POINT INTEGRATION

In general, we wish to evaluate integrals over the BZ in the form

$$I=\int_{\mathrm{BZ}} f(\mathbf{k})z(E_f-E(\mathbf{k}))d\mathbf{k}\ ,$$
$$z(E_f-E(\mathbf{k}))=\int_{-\infty}^{E_f}\delta(\epsilon-E(k))d\epsilon\ . \tag{A1}$$

In the Gaussian smearing technique the δ function is broadened into a Gaussian with variance w. By using a sufficiently large w, one immediately improves the k-sum convergence. However, the only justification for this *ad hoc* procedure is that in the limit $w\rightarrow 0$ one would recover the absolutely converged result at the expense of using a prohibitively fine mesh. Thus for each choice of w the k sum converges to a different result, and the convergence with respect to w must be further checked. Methfessel and Paxton[32] suggested a more efficient way to achieve absolute convergence. They expand the δ function in Eq. (1) as $\delta(x)=\sum_{n=0}^{\infty}A_n H_{2n}e^{-x^2}$, where $x=[\epsilon-E(\mathbf{k})]/w$, H_{2n} are Hermite polynomials, A_n are the expansion coefficients, and w is an arbitrary "linewidth." By truncating the sum in the expansion of the δ function. The order $n=0$ corresponds to the simple Gaussian broadening. It can be proved[59] that the energy $E(n,w)$ at convergence in the k sum for fixed n and w tends to the true energy E_0 as $E(n,w)\rightarrow E_0+o((w/E_f)^{2n+1})$, i.e., by increasing n one reaches E_0 at a larger w. Since by increasing w the number of k points necessary to reach convergency (for the assigned w) decreases, the convergence to the correct result is obtained with fewer k points, for a suitable choice of w and n, than in the simple Gaussian scheme.

*Present address: Max Planck Institut für Festkörperforschung, Postfach 8006565, Stuttgart, D-70506 Germany.
[1]L. Bosio, J. Chem. Phys. **68**, 1221 (1978).
[2]L. Bosio, A. Defrain, H. Curien, and A. Rimsky, Acta Crystallogr. B **25**, 995 (1969).
[3]L. Bosio, H. Curien, M. Dupont, and A. Rimsky, Acta Crystallogr. B **28**, 1974 (1972).
[4]L. Bosio, H. Curien, M. Dupont, and A. Rimsky, Acta Crystallogr. B **29**, 367 (1973).
[5]R. W. G. Wyckoff, *Crystal Structures,* 2nd. ed. (Wiley, New York, 1962), Vol. I, p. 22. A word of caution is in order: Of the six possible ways to assign *a, b, c* to the three crystal axes, at least three different versions can be found in literature.
[6]V. Heine, J. Phys. C **1**, 222 (1968).
[7]J. E. Inglesfield, J. Phys. C **1**, 1337 (1968).
[8]R. D. Etters, in *Simple Molecular System at Very High Pressures,* Vol. 186 of *NATO Advanced Study Institute, Series B: Physics,* edited by A. Polian, P. Loubeyre, and N. Beccara (Plenum, New York, 1989), p. 108.
[9]R. O. Jones, J. Chem. Phys. **99**, 1194 (1993).
[10]R. W. Powell, M. J. Woodman, and R. P. Tye, Br. J. Appl. Phys. **14**, 432 (1963).
[11]O. Hundery and R. Ryberg, J. Phys. F **4**, 2084 (1974).
[12]R. Kofman, P. Cheyssac, and J. Richard, Phys. Rev. B **16**, 5216 (1977).
[13]F. Greuter and P. Oelhafen, Z. Phys. B **34**, 123 (1979).
[14]D. J. Stroud and M. J. Scott, J. Phys. F **5**, 1667 (1975).
[15]W. A. Reed, Phys. Rev. **188**, 1184 (1969).
[16]R. Griessen, H. Krugmann, and H. R. Ott, Phys. Rev. B **10**, 1160 (1974).
[17]A. R. Ubbelohde, *The Molten State of Matter* (Wiley, New York, 1978).
[18]Y. Waseda, *The Structure of Non-Crystalline Materials* (McGraw-Hill, New York, 1980), p. 54.
[19]X. G. Gong, G. L. Chiarotti, M. Parrinello, and E. Tosatti, Europhys. Lett. **21**, 469 (1993).
[20]X. G. Gong, G. L. Chiarotti, M. Parrinello, and E. Tosatti, Phys. Rev. B **43**, 14 277 (1991).
[21]J. Hafner and W. Jank, Phys. Rev. B **42**, 11 530 (1990).
[22]J. P. Perdew and A. Zunger, Phys. Rev. B **23**, 5048 (1981).
[23]L. Kleinman and M. D. Bylander, Phys. Rev. Lett. **48**, 1425 (1982).
[24]R. Stumpf, X. Gonze, and M. Scheffler (unpublished).
[25]S. G. Louie, S. Froyen, and M. L. Cohen, Phys. Rev. B **26**, 1738 (1982).
[26]U. von Barth and R. Car (unpublished).
[27]We thank A. Dal Corso and P. Giannozzi for providing us the code for the generation of the pseudopotential.
[28]A. D. Becke, Phys. Rev. A **38**, 3098 (1988).
[29]J. P. Perdew, Phys. Rev. B **33**, 8822 (1986).
[30]G. Ortiz, Phys. Rev. B **45**, 11 328 (1992).
[31]G. Ortiz and P. Ballone, Phys. Rev. B **43**, 6376 (1991).
[32]M. Methfessel and A. T. Paxton, Phys. Rev. B **40**, 3616 (1989).
[33]C. L. Fu and K. M. Ho, Phys. Rev. B **28**, 5480 (1983).
[34]R. P. Feynman, Phys. Rev. **56**, 340 (1939).
[35]O. H. Nielson and R. M. Martin, Phys. Rev. **32**, 3780 (1985); **32**, 3792 (1985).
[36]L. F. Vereshchagin, S. S. Kabalkina, and Z. V. Toritskaya, Dokl. Akad. Nauk. SSSR **158**, 1061 (1965) [Sov. Phys. Dokl. **9**, 894 (1965)].
[37]A. Bererhi, A. Bosio, and R. Cortes, J. Non-Cryst. Solids **30**, 253 (1979).
[38]W. Bückel and R. Hilsch, Z. Phys. **138**, 461 (1975); J. Berty, M. J. David, and L. Lafourcade, J. Chim. Phys. **74**, 952 (1977).
[39]C. E. Weir, G. J. Piermarini, and S. Block, J. Chem. Phys. **54**, 2768 (1971).
[40]F. D. Murnaghan, Proc. Nat. Acad. Sci. U. S. A. **30**, 244 (1944).
[41]K. R. Lyall and J. F. Cochran, Can. J. Phys. **49**, 1075 (1971).
[42]The structural parameters of α-Ga have also been calculated with the pseudopotential of Bachelet *et al.* (Ref. 43) with similar results: $V_{eq}=116$, $a=8.17$, $b/a=1.001$, $c/a=1.7$, $u=0.081\,08$, $v=0.156\,36$, $B=701$ kbar, and $b'=4.868$.
[43]G. B. Bachelet, D. R. Hamann, and M. Schlüter, Phys. Rev. B **26**, 4199 (1982).
[44]C. Regnaut, J. P. Badiali, and M. Dupont, J. Phys. (Paris) Colloq. **41**, C8-604 (1980).
[45]We take the Debye temperature of GaII 40% lower than that of α-Ga (Ref. 55).
[46]The properties of the Ga_2 molecule have recently been studied by Jones (Ref. 9) in the LDA with the same KB pseudopotential used by us. The LDA interatomic distance of the molecule in the electronic ground state $^3\Sigma_u$ is 4.864 a.u. The experimental interatomic distance is not known, but the LDA value is indeed 7% smaller than the value obtained with an all-electron quantum chemistry calculation [complete active space self-consistent field followed by second-order configuration interactions (CI)] (Ref. 47). The quantum-chemistry calculation of Ref. 47 is actually not a full CI, and the LDA vibrational frequency is 184 cm^{-1}, closer to experiment (184 cm^{-1}) than the quantum-chemistry value (154 cm^{-1}). Thus, the accuracy of the LDA for the Ga_2 molecule is unclear and should be further investigated by comparison with more accurate CI calculations.
[47]K. Balasubramanian, J. Phys. Chem. **94**, 7764 (1990).
[48]M. Bernasconi, S. De Gironcoli, G. L. Chiarotti, and E. Tosatti (unpublished).
[49]J. P. Perdew, J. A. Chevary, S. H. Vosko, K. A. Jackson, M. R. Pederson, D. J. Singh, and C. Fiolhais, Phys. Rev. B **46**, 6671 (1992).
[50]M. T. Yin and M. L. Cohen, Phys. Rev. B **26**, 5668 (1982).
[51]O. Jepsen and O. K. Andersen, Solid State Commun. **9**, 1763 (1971); H. L. Skriver *The LMTO Method* (Springer-Verlag, Berlin, 1984), p. 194.
[52]J. Zak, *Irreducible Representations of Space Groups* (Benjamin, New York, 1969).
[53]S. Gottlicher and E. Wolfel, Z. Electrochem. **63**, 891 (1959).
[54]W. Reichardt, R. M. Nicklow, G. Dolling, and H. G. Smith, Bull. Am. Phys. Soc. **14**, 378 (1969); P. H. Dederichs, H. Schober, and D. J. Sellnyer, in *Metals: Phonons and Electron States. Fermi Surfaces,* Landolt-Börnstein, New Series III/13a, edited by K.-H. Hellwege and J. L. Olsen (Springer-Verlag, Berlin, 1981), p. 59.
[55]L. Bosio, R. Cortes, J. R. D. Copley, W. D. Teuchert, and J. Lefebvre, J. Phys. F **11**, 2261 (1981).
[56]O. Züger and U. Dürig, Phys. Rev. B **46**, 7319 (1992); O. Züger, Ph. D. thesis, ETH Zurig, 1992; O. Züger and U. Dürig, Ultramicrosc. **42**, 520 (1992).
[57]M. Bernasconi, G. L. Chiarotti, and E. Tosatti, Phys. Rev. Lett. **70**, 3295 (1993); Surf. Sci. **307-309**, 936 (1994).
[58]M. Bernasconi, G. L. Chiarotti, and E. Tosatti, following paper, Phys. Rev. B **52**, 9999 (1995).
[59]A. De Vita, Ph. D. thesis, Keele University, 1992 (unpublished). We are grateful to S. De Gironcoli for pointing out this result to us.